Available online at www.sciencedirect.com
SCIENCE DIRECT®
Biochemical and Biophysical Research Communications 325 (2004) 48–58
BBRC
www.elsevier.com/locate/ybbrc

Age-related compensatory activation of pyruvate dehydrogenase complex in rat heart

Régis Moreau[a], Shi-Hua D. Heath[a], Catalin E. Doneanu[b,1], Robert A. Harris[c], Tory M. Hagen[a,d,*]

[a] Linus Pauling Institute, Oregon State University, Corvallis, OR 97331-6512, USA
[b] Department of Chemistry, Oregon State University, Corvallis, OR 97331-4003, USA
[c] Department of Biochemistry and Molecular Biology, Indiana University School of Medicine, Indianapolis, IN 46202-5122, USA
[d] Department of Biochemistry and Biophysics, Oregon State University, Corvallis, OR 97331-6512, USA

Received 4 September 2004

Abstract

Mitochondrial uptake and β-oxidation of long-chain fatty acids are markedly impaired in the aging rat heart. While these alterations would be expected to adversely affect overall pyridine nucleotides, NADH levels do not change significantly with age. This conundrum suggests that specific compensatory mechanisms occur in the aging heart. The comparison of cardiac pyruvate dehydrogenase complex (PDC) kinetics in 4- and 24- to 28-month-old F344 rats revealed a 60% significant increase in V_{max} with no change in PDC expression, and a 1.6-fold decrease in the Michaelis constant (K_m) in old compared to young rats. The observed kinetic adjustments were selective to PDC, as neither the V_{max} nor K_m of citrate synthase changed with age. PDC kinase-4 mRNA levels decreased by 57% in old vs young rat hearts and correlated with a 45% decrease in PDC phosphorylation. We conclude that PDC from old rat hearts catabolizes pyruvate more efficiently due to an adaptive change in phosphorylation.

Keywords: Aging; Mitochondria; Heart; Myocardium; Energetics; Kinetics; Pyruvate dehydrogenase; NADH; ATP

There is compelling evidence that age-related mitochondrial decay contributes to myocardial dysfunction, including stiffness, apoptosis, atrophy, and compensatory hypertrophy [1–6]. To maintain myocardial integrity and function, a constant supply of high-energy phosphates is required since little reserves are maintained. Production of high-energy phosphates depends on the effective conversion of long-chain fatty acids and carbohydrates to reduced pyridine nucleotides (NADH) generated in the mitochondria via β-oxidation, pyruvate oxidation, and the citric acid cycle.

There is increasing evidence that mitochondrial bioenergetics is markedly impaired in the aging rat heart. In particular, both pyruvate and long-chain fatty acid uptake by mitochondria decline by 30–40% [7–10], thus affecting raw fuel availability for ATP production. Fatty acid oxidation provides 40–50% of the acetyl-CoA generated by the heart [11]. The transport of fatty acids (as activated CoA ester) into the mitochondrial matrix for β-oxidation is a complex process involving several enzymes (two transferases and one translocase), co-substrates (CoA and carnitine), and the crossing of two membranes. Aging of the myocardium is associated with declines of carnitine palmitoyl transferase-1 (CPT-1) activity in the outer mitochondrial membrane

* Corresponding author. Fax: +1 541 737 5077.
E-mail address: tory.hagen@oregonstate.edu (T.M. Hagen).
[1] Present address: Department of Medicinal Chemistry, University of Washington, Box 357610, Seattle, WA 98195-7610, USA.

0006-291X/$ - see front matter © 2004 Elsevier Inc. All rights reserved.
doi:10.1016/j.bbrc.2004.10.011

and carnitine–acylcarnitine translocation across the inner membrane [9]. 3-Hydroxyacyl-CoA dehydrogenase activity, often taken as an index of the capacity of the heart for β-oxidation, also decreases by ~30% in old rat hearts [12,13]. While transport capacity may be sufficient to compensate for a partial inhibition of pyruvate uptake [14], the lesions affecting long-chain fatty acid transport and oxidation remain substantial. Thus, these alterations would be expected to adversely affect steady-state NADH levels and consequently impair electron flux through the mitochondrial electron transport chain. However, despite the consensus that mitochondrial function declines in the aging heart, there is no evidence that myocardial ATP levels or energy charge is compromised. This suggests that the heart in general and mitochondria in particular adapt to these adverse changes and maintain overall cardiac bioenergetics. One aspect of such compensation is an increased reliance on glucose oxidation for ATP synthesis to make up for limited long-chain fatty acid catabolism in the aging myocardium [9]. The pyruvate dehydrogenase complex (PDC) is hypothesized to play a major role in this compensatory mechanism because it represents the prevailing pathway for entry of carbohydrates into the citric acid cycle [11]. PDC, a mitochondrial multienzyme complex that catalyzes the conversion of pyruvate to acetyl-CoA [15], is rate-limiting for glucose oxidation in the myocardium and central to the bioenergetics of aerobic tissues, including the heart. PDC is one of the principal means to regenerate the mitochondrial pool of reduced pyridine nucleotides and to control their flux to the electron transport chain. At fixed concentrations of substrate, the flux through PDC will be proportional to the activity of the enzyme. In the present study, we evaluated the role of cardiac PDC in opposing the decline in bioenergetics by measuring its activity at various substrate concentrations, its protein content, and the status of PDC-associated kinase and phosphatase.

The present study provides new evidence suggesting that PDC plays an important role in maintaining adequate NADH levels in the aging F344 rat heart. Heart PDC of 24- to 28-month-old rats exhibits altered kinetic characteristics (higher V_{max}, lower K_m, resiliency toward competitive inhibitor) consistent with an improved catalytic efficiency, thereby compensating for the declining pyruvate availability.

Materials and methods

Animals and diets. Rats (Fischer 344, male, albino), both young (4 months) or old (24–28 months) from the National Institute on Aging, were housed in cages in a controlled environment (temperature 22 ± 2 °C, 12:12-h light–dark cycle) and fed AIN-93M diet (Dyets, Bethlehem, PA) ad libitum for 2 weeks. Animals had free access to food and water until sacrifice.

Free CoA and short-chain CoA esters. Free CoA, acetyl-CoA, succinyl-CoA, and malonyl-CoA levels were determined by HPLC, as described previously [16] with minor modifications. Rats were anesthetized with diethyl ether, a midlateral incision was made in the chest, the heart was removed, and a portion was frozen in liquid nitrogen and stored at −80 °C for up to 2 months until analysis. Frozen tissue was homogenized using a Potter–Elvehjem homogenizer (5 strokes, 0.1 g tissue/ml homogenization solution) in an ice-cold solution containing 5% (w/v) sulfosalicylic acid, 50 μM dithioerythritol (pH 2), and 20 μM methylmalonyl-CoA (internal standard). After centrifugation (2000*g* for 10 min at 4 °C) the supernatant was collected, filtered through 0.22-μm nylon syringe filters, and a 50-μl aliquot was injected onto a Supelcosil LC-18-DB (15 × 4.6 mm, 3-μm particle size) column (Supelco, Bellefonte, PA). Separation was achieved using HPLC at room temperature with a flow rate of 1.3 ml/min. Solvents and conditions for separation were as follows: Solvent A (100 mM monobasic Na^+ phosphate, 75 mM Na^+ acetate, pH 4.6) and Solvent B (70% Solvent A in methanol); 0 min, 90% A; 10 min, 60% A; and 17.6 min, 10% A. The HPLC system consisted of Waters 2690 Separations Module (Waters, Milford, MA) coupled to Waters 2487 Absorbance Detector set at 254 nm. Data were acquired using Millenium^{32} 4.0 software for Waters. Free CoA, acetyl-CoA, succinyl-CoA, and malonyl-CoA were identified relative to standards (Sigma, St. Louis, MO) and quantified by comparing the recovery-corrected peak area with that of the standard. Recovery of internal standard methylmalonyl-CoA averaged 89 ± 3%.

Isolation of mitochondria. Rat heart mitochondria were isolated as described previously [17]. Briefly, rats were anesthetized with diethyl ether, a midlateral incision was made in the chest, and the heart was removed and minced in cold 0.3 M mannitol containing 5 mM Mops, 5 mM KH_2PO_4, 1 mM $CaCl_2$, and 0.1% BSA (fatty acid-free, fraction V, Calbiochem–Novabiochem, La Jolla, CA), pH 7.4. Minced heart was subjected to collagenase treatment (Type IV, Sigma) at 4 °C for 40 min whereupon digestion was stopped with EGTA and the buffer decanted. The heart digest was homogenized using a Potter–Elvehjem homogenizer in 8 volumes of cold 0.3 M mannitol, 5 mM Mops, 5 mM KH_2PO_4, 1 mM EGTA, 0.1 mM *n*-tosyl-L-phenylalanine chloromethyl ketone, aprotinin (8 TIU/L), 0.5 μM leupeptin, 0.5 μM pepstatin A, and 0.1% BSA (fatty acid-free), pH 7.4. The homogenate was then centrifuged at 1500*g* for 10 min at 4 °C. The supernatant was further centrifuged at 10,000*g* for 10 min at 4 °C. The resulting pellet was washed twice by centrifugation at 10,000*g* for 10 min at 4 °C and resuspended to a final concentration of 15 mg protein/ml. This crude preparation is enriched in subsarcolemmal mitochondria, but also contains interfibrillary mitochondria as well. Protein content was determined using the bicinchoninic acid method (Pierce, Rockford, IL) with BSA as a standard.

Pyruvate dehydrogenase complex activity and kinetics. Pyruvate dehydrogenase complex (PDC) activity was determined spectrophotometrically using a 96-well plate reader (SpectraMax, Molecular Dynamics, Sunnyvale, CA) by monitoring the reduction of NAD^+ at 340 nm for 10 min at 30 °C. The assay mixture was composed of 2 mM NAD^+, 0.6 mM thiamine pyrophosphate, 0.24 mM CoASH, 0.1 mM DTT, 5 mM dichloroacetate (a PDK inhibitor), 25 mM potassium fluoride (a PDP inhibitor), 25 mM oxamate (a lactate dehydrogenase inhibitor [18]), 1 mM $MgCl_2$, 20 μM $CaCl_2$, and 2 mM pyruvate (concentration near saturation) in 50 mM Tris–HCl, pH 7.6; and 20 μg mitochondrial proteins solubilized with *n*-octyl β-D-glucopyranoside (0.15% [w/v] in 50 mM Tris–HCl, pH 7.6). Kinetic parameters were assessed using the same protocol but varying the pyruvate concentration (0.2–4 mM). Given the hyperbolic profile of the initial velocity as a function of pyruvate concentration, the PDC-catalyzed reaction was considered to follow Michaelis–Menten kinetics. The apparent K_m (K_m^{app}) for pyruvate was determined by varying the concentration of fluoropyruvate, a specific inhibitor of PDC, from 20 to 100 μM. Kinetic characteristics (K_m, K_m^{app}, V_{max}, and K_m^{app}/V_{max}) were obtained graphically. The initial velocity was determined from the linear portion

of the curve and plotted using the Lineweaver–Burk double-reciprocal representation.

Western blotting. Frozen crude mitochondria were solubilized in PBS containing 0.1% (v/v) Triton X-100 mixed with sample buffer (125 mM Tris–HCl, pH 6.8, 4% [w/v] SDS, 20% [v/v] glycerol, 2% [v/v] β-mercaptoethanol, and 0.02% [w/v] bromophenol blue), and then heat denatured (95 °C, 5 min). The protein (70 μg) was subjected to reducing SDS–PAGE, followed by electroblotting onto nitrocellulose membranes and incubated with antibodies to PDC or porcine lipoamide dehydrogenase (Rockland, Gilbertsville, PA) in blocking buffer (20 mM Trizma base, 150 mM NaCl, 0.1% [v/v] Tween 20, 5% [w/v] non-fat dried milk, and 0.5% [w/v] BSA, pH 7.5). Membranes were rinsed three times for 10 min and incubated with horseradish peroxidase-conjugated secondary antibodies. Antibody binding was visualized using an ECL Western Blotting System (Amersham–Pharmacia Biotech, Piscataway, NJ), and band density was quantified using an AlphaImager imaging system (Alpha Innotech, San Leandro, CA).

Nano-LC ESI MS/MS. To validate the position of rat heart PDC components on Western blots, rat heart PDC was compared side-by-side with purified porcine heart PDC. Polypeptides contained in the porcine heart PDC preparation (Sigma) were identified by using a nanoscale liquid chromatography system coupled to electrospray ionization tandem mass spectrometry (nano-LC ESI M/MS). Polypeptides were separated by 7.5% SDS–PAGE under reducing conditions and stained with Coomassie blue R-250. Three prominent bands were removed from the gel, destained in 5% methanol/7% acetic acid, washed with 100 mM NH_4HCO_3, dehydrated with acetonitrile, and dried under vacuum before digestion with modified porcine trypsin (Promega, Madison, WI) in 50 mM ammonium bicarbonate, 5 mM calcium chloride, overnight at 37 °C. Five microliters of the peptide digest was injected onto a 25-cm long PicoFrit column (New Objective, Cambridge, MA) packed with 5-μm particle Luna C_{18} silica (Phenomenex, Torrance, CA), and separated using a gradient of acetonitrile supplemented with 0.1% acetic acid and 0.01% trifluoroacetic acid delivered at a flow rate of 0.3 μl/min [19]. Nano-LC ESI MS/MS analyses were performed on a LC-Quadrupole ion trap mass spectrometer (Thermo Finnigan, San Jose, CA). The LC-Quadrupole was operated in the MS mode with the spray potential set at 2.5 kV, the inlet capillary heated to 180 °C, the capillary potential set at 46 V, and a maximum injection time of 50 ms. The instrument was set to acquire a full MS scan between 400 and 2000 m/z followed by a MS/MS scan. For operation in the MS/MS mode, the maximum injection time was increased to 500 ms, the isolation width set to 1 Da, and the collision energy set to 30% with a 30-ms activation time. Using a data dependent algorithm, the first most intense ion ($>2 \times 10^4$ counts) was selected for MS/MS. To identify peptide fragments, MS/MS spectra were compared to the NCBI protein database using the Sequest software (Thermo Finnigan, San Jose, CA).

PDC phosphorylation state. Heart mitochondria were isolated as described above in the presence of 5 mM dichloroacetate, and 25 mM potassium fluoride, and 15 μg mitochondrial proteins were size separated by 10% SDS–PAGE under reducing conditions. Proteins were transferred to PVDF membrane using a transfer buffer free of SDS (25 mM Trizma base, 192 mM glycine, and 10% [v/v] methanol). Fluorescent staining of PVDF membrane was performed with Pro-Q Diamond phosphoprotein blot stain (Molecular Probes, Eugene, OR) according to the manufacturer's instructions. Ovalbumin (45 kDa, 2 phosphate groups) was used as a positive control, while BSA (66 kDa) was used as a negative control. Following destaining and air-drying, the membrane was imaged using a FMBIO II fluorescence scanner (Hitachi America, New York, NY) operated with a 20-mW laser excitation source set at 532 nm and collection at 585 nm. Following image acquisition, the membrane was probed for the E1α component of PDC by Western blotting using specific monoclonal antibodies to human E1α (Molecular Probes) in blocking buffer (20 mM Trizma base, 150 mM NaCl, 0.2% [v/v] Tween 20, and 0.5% [w/v] BSA, pH 7.5). Data are reported as the ratio of phosphorylated E1α :total E1α. Band density was determined using an AlphaImager imaging system (Alpha Innotech).

Pyruvate dehydrogenase kinase activity and content. Pyruvate dehydrogenase kinase (PDK) activity was measured as the linear, initial rate of phosphorylation of semi-purified porcine PDC (Sigma) catalyzed by PDK contained in crude mitochondrial fractions freshly isolated from young and old rats. Because PDK will phosphorylate the E1α component (44 kDa) of PDC, this subunit was resolved using 10% SDS–PAGE. The reaction mixture (30 μl final volume) consisted of 3 μg protein of heat-denatured porcine PDC, 9.5 μg mitochondrial protein, 25 mM potassium fluoride, 1 mM EDTA, 1 mM dithiothreitol, 2 mM $MgCl_2$, 0.15 mM cold ATP, and 3 μCi [γ-^{32}P]ATP (3 Ci/mol, Amersham–Pharmacia Biotech) in 50 mM Mops, pH 7.5. Incubation took place at 30 °C for 20 min, whereupon the reaction was stopped by adding 7.5 μl sample buffer (250 mM Tris–HCl, pH 6.8, 720 mM β-mercaptoethanol, 10% [w/v] SDS, 50% [v/v] glycerol, and 0.05% [w/v] bromophenol blue).

PDK-1 content in hearts of young and old rats was determined by Western blotting as described above using antibodies to human PDK-1 (Calbiochem–Novabiochem, San Diego, CA). Lipoamide dehydrogenase was used as loading control.

PDK-2, PDK-4, pyruvate dehydrogenase phosphatase-1, and pyruvate dehydrogenase phosphatase-2 mRNA levels. While pyruvate dehydrogenase phosphatase-1 (PDP-1) mRNA level was determined by using two methods, i.e., duplex RT-PCR and real-time RT-PCR, pyruvate dehydrogenase phosphatase-2 (PDP-2), PDK-2, and PDK-4 mRNA levels were determined by real-time RT-PCR only. In all cases, total RNA was extracted from myocardium using the SV Total RNA Isolation System (Promega, Madison, WI) and the first DNA strand synthesized using the RETROscript kit (Ambion, Austin, TX). For PDP-1, the target DNA was amplified by PCR using two sets of synthetic oligonucleotide primers (duplex PCR: forward 5′CTTCTACGCCTCAGAAATTT TACCT, reverse 5′CATTCTGAGCATT GTGGTCATTAG; real-time PCR: forward 5′AAGAGCGTGGTAAAGCAGGA, reverse 5′CT GTGGCCTTAATCGGTGAT) that amplify a 741 and 225-bp fragment, respectively, of rat PDP-1 (GenBank AF062740). The 741-bp amplified fragment was purified by agarose electrophoresis and sequenced using an ABI PRISM 377 DNA sequencer (Applied Biosystems, Foster City, CA). Automated DNA sequencing confirmed that the PCR product was identical to the intended template. Duplex PCR was carried out using a QuantumRNA 18S Internal Standards kit (Ambion, Austin, TX) and 3 μCi as [α-^{32}P]dCTP (Amersham–Pharmacia Biotech) per reaction. Quantifications were performed by scanning densitometry of the autoradiographs. Real-time PCR was performed by using the DNA Engine Opticon 2 system (MJ Research, Waltham, MA) and DyNAmo SYBR Green pPCR Kit (Finnzymes Oy, Espoo, Finland) according to the manufacturer's instructions. To quantify gene expression a 205-bp fragment of rat β-actin (GenBank NM_031144) was concurrently amplified (forward 5′CCTTCCTTCCTGGGTATG GAATCC, reverse 5′GAGCAATGATCTTGATCTTCATGGTG) and used as an internal standard. Real-time PCR was repeated using specific primers for rat PDP-2 (GenBank AF062741, forward 5′GTGGAAGACCGACAAGGTGT, reverse 5′CTTCCTCCATC TGCTCCAAG), rat PDK-2 (GenBank BC061823, forward 5′AGGAAGTCAATGGCACCAAC, reverse 5′TTTGATTGGGAG GGAGAGTG), rat PDK-4 (GenBank AF034577, forward 5′CCTTT GGCTGGTTTTGGTTA, reverse 5′CACCAGTCATCAGCCTC AGA), and β-actin as a standard. Amplicon authenticity was confirmed by agarose gel electrophoresis and melt curve analysis. PCR efficiencies were assessed with serial dilutions of the template (0.001, 0.01, 0.1, 1, 10, and 100 ng cDNA/reaction) and 0.3 μM of each primer, and plotting threshold cycle (C_T) versus log amount of template. Since PCR efficiencies between target genes and β-actin were comparable, unknown amounts of target in the sample were normalized by comparing the C_T values with the internal standard β-actin.

Citrate synthase activity and kinetics. Citrate synthase (CS) activity was determined spectrophotometrically using a SpectraMax 96-well

plate reader (Molecular Dynamics). The reaction mixture consisted of 0.1 M Tris–HCl, pH 8.0; 0.4 mM acetyl-CoA; 0.5 mM oxaloacetate; 0.1 mM 5,5′-dithiobis-2-nitrobenzoic acid (DTNB); and 10 μg mitochondrial protein. The reduction of DTNB ($\varepsilon = 16{,}440\ M^{-1}\ cm^{-1}$) was followed at 412 nm for 2 min at 30 °C with the spectra corrected by subtracting any absorbance at 360 nm. Deacylase activity was estimated by omission of oxaloacetate. A reaction blank was performed where heat-denatured (95 °C, 5 min) mitochondria were used in the assay. One CS unit equals 1 mmol DTNB reduced per minute at 30 °C. Kinetic analysis was determined using the same protocol but varying acetyl-CoA concentration (0.025–0.4 mM). The velocity was determined from the linear portion of the curve and plotted according to Lineweaver–Burk double-reciprocal representation. The Michaelis constant (K_m) was obtained graphically from computer-generated least-squares fit.

Statistical analysis. Data were analyzed by unpaired two-tailed Student's *t* test and least-square regression using the Statview package (SAS Institute, Cary, NC). Proportions were arcsine transformed prior to analysis. All statistical tests were performed to the 95% level of confidence.

Results

Short-chain CoA esters

In the heart, short-chain CoA esters are mostly generated by mitochondrial bioenergetics. Thus, changes in the cellular content of these intermediates can reflect the disharmony of cellular aerobic metabolism. To illustrate the age-related decline in mitochondrial bioenergetics of the heart, we determined the steady-state levels of free CoA and its short-chain esters in young and old rats. As expected, free CoA, acetyl-CoA, and succinyl-CoA levels were significantly ($P \leqslant 0.05$) lower (by ~30%) in old rat hearts (Fig. 1A). The levels of malonyl-CoA, a potential regulator of long-chain fatty acid metabolism, were 14% lower in old rats (3.57 ± 0.50 nmol g^{-1} tissue) than in young rats (4.15 ± 0.87 nmol g^{-1} tissue), but the difference was not significant ($P = 0.275$, Fig. 1A). Malonyl-CoA levels in the heart were correlated ($r = 0.699$, $P = 0.036$) with acetyl-CoA levels, suggesting that malonyl-CoA is derived from acetyl-CoA (Fig. 1B). The CoA:acetyl-CoA ratio, often taken as an indicator of long-chain fatty acid flux to produce mitochondrial acetyl-CoA, was not significantly ($P = 0.672$) affected by age (Fig. 1C). This suggests that both CoA and acetyl-CoA levels decreased to a comparable extent in old rat hearts. Overall, the decline in these intermediates agrees with the age-associated loss of substrate uptake (fatty acid and pyruvate) by heart mitochondria.

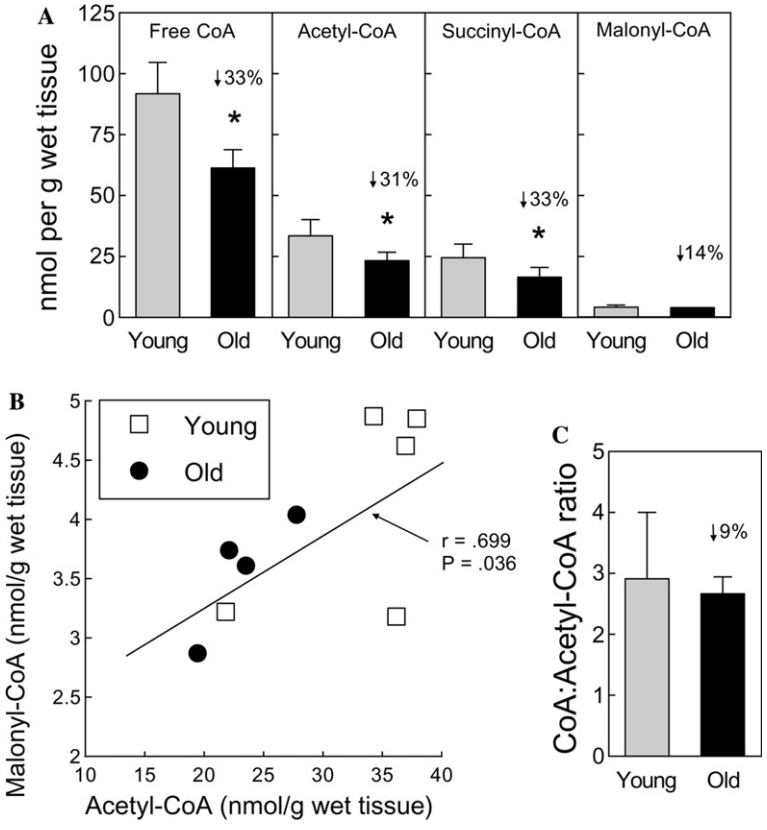

Fig. 1. Steady-state levels of $CoAS^-$ and short-chain CoA esters in the hearts of young and old F344 rats. (A) Free $CoAS^-$, acetyl-CoA, and succinyl-CoA concentrations decreased significantly (*$P \leqslant 0.05$) by 33%, 31%, and 33%, respectively, in old rat hearts compared to their young counterparts. (B) Correlation between heart malonyl-CoA and acetyl-CoA was assessed by linear regression. (C) The levels of malonyl-CoA and free CoA:acetyl-CoA ratio did not differ significantly between age groups. Data are shown as means ± SD for 4–5 animals per age class.

PDC activity and content

It has been shown that the aging rat heart compensates for the decline in long-chain fatty acid oxidation by increasing the use of exogenous glucose [9] via its glycolytic product, pyruvate. While increasing pyruvate flux through the mitochondrial pyruvate dehydrogenase complex (PDC) improves cardiac function during ischemic episodes, pyruvate flux may not be sufficient because the aging heart suffers a decline in pyruvate uptake. Thus, we sought to determine whether aging adversely affected PDC activity in rat heart. For this purpose, PDC activity was measured in the crude mitochondrial fraction after inhibiting both PDC kinase and phosphatase with dichloroacetate and potassium fluoride, specific inhibitors of these respective enzymes. Results showed that PDC activity was significantly ($P < 0.01$) higher (by ~60%) in old (27.9 ± 4.3 nmol NADH min^{-1} mg^{-1} protein) compared to young (17.4 ± 3.8 nmol NADH min^{-1} mg^{-1} protein) rat hearts (Fig. 2A).

To determine whether increased PDC activity in old rat hearts was due to increased enzyme levels, the content of PDC components (E1α, E1β, E2, and E3) was determined by Western blotting. The antiserum used cross-reacts with PDC components from both pig and rat hearts. Under these conditions, the E3-binding protein (BP) could not be separated electrophoretically from E3. The position of pig PDC components as resolved by SDS–PAGE was ascertained by proteomic analyses of the bands using a nano-LC ESI MS/MS and Sequest search to match amino acid sequence tags with the NCBI protein database (Table 1). These data were used to establish the position of PDC components from rat heart mitochondria (Fig. 2B). When comparing the PDC content from young and old rats, the results indicated there was no significant difference in the amount either of E1α, E1β, E2 or E3 enzyme (Fig. 2C). Thus, PDC activity increased in old rats with no change in enzyme content, suggesting an alternative explanation.

PDC phosphorylation state

PDC activity is, in part, controlled by phosphorylation/dephosphorylation, where a specific pyruvate dehydrogenase kinase (PDK) phosphorylates three serine residues of E1α-PDC, thereby inactivating pyruvate oxidation. We determined the extent of E1α-PDC phosphorylation in rat hearts by fluorescent staining of mitochondrial proteins with Pro-Q Diamond followed by Western blotting for E1α. Results showed an age-related 45% decrease ($P < 0.01$) in phosphorylated E1α (Figs. 3A and B) among fed rats, which is reversed after 24-h starvation. A change in PDC phosphorylation may result from alteration to PDK and PDP status.

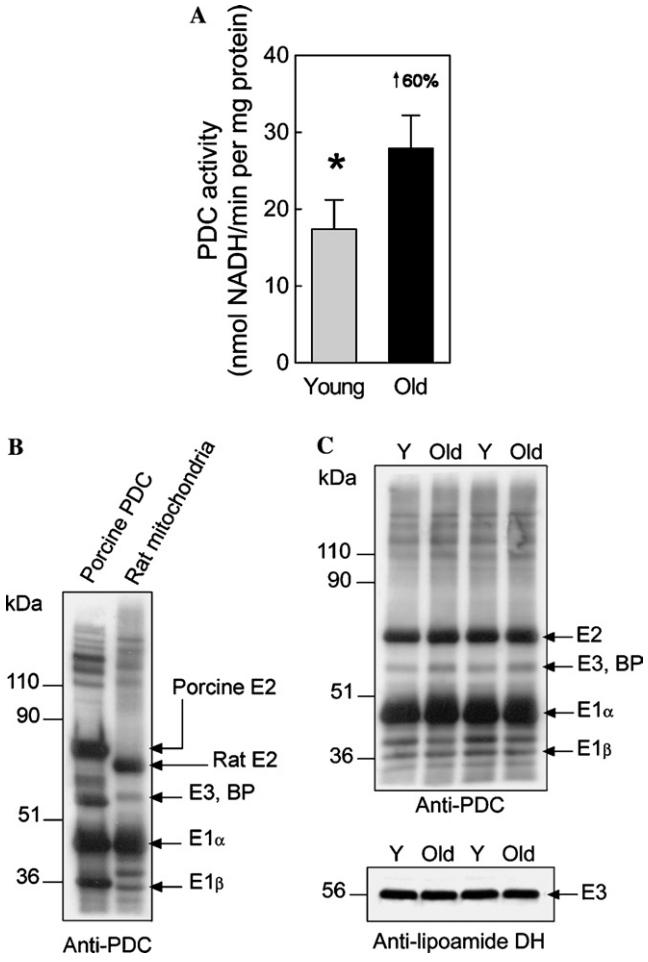

Fig. 2. Age-related changes to cardiac PDC activity and content in rats. PDC activity and content were measured in isolated mitochondria. (A) Old rats exhibit significantly higher (up by 60%, $*P < 0.01$) PDC activity than young rats. Data are shown as means ± SD for 5 animals per age class. (B) Heart mitochondrial proteins were separated by 7.5% SDS–PAGE, transferred to nitrocellulose membrane, and immunoblotted with anti-human PDC antibodies. The identity of the bands was confirmed based on the co-separation of purified porcine PDC and oligopeptide sequence analyses of the most intense bands by mass spectrometry (see Table 1). (C) Western blotting analyses of rat heart mitochondria, using antibodies to human PDC and porcine lipoamide dehydrogenase (the E3 component of PDC), showed no change in the contents of PDC enzymatic components, i.e., E1α, E1β, E2, E3, or E3-binding protein (BP).

PDK and PDP status

In cardiac muscle, E1α phosphorylation is catalyzed by three highly specific PDK isoforms (PDK-1, PDK-2, and PDK-4), which leads to the complete inactivation of PDC. Among the PDK isoforms found in rodents, PDK-1 is predominantly expressed in cardiac muscle followed by PDK-2 and PDK-4. Therefore, elevated PDC activity may result from lowered phosphorylation state of the enzyme stemming from changes in PDK activity. Mitochondria isolated from young and

Table 1
Identification of the enzyme components of porcine heart pyruvate dehydrogenase complex (PDC) using amino acid sequence tags obtained from nano-LC ESI MS/MS analyses[a]

Identified protein	NCBI No.	Molecular mass (Da)[b]	Sequence coverage (%)	Peptide sequence	Position
Dihydrolipoamide acetyltransferase (E2 component of PDC)	14587786	68,991	8	ILVAEGTR	148–155
				ILIPEGTR	275–282
				GIDLTQIK	369–376
				DIDSFVPTK	388–396
				ISVNDFIIK	474–482
				LFPADNEK	597–604
Pyruvate dehydrogenase (E1α component of PDC)	448580	40,315	20	FANDATFEIK	1–10
				LEEGPPVTTVLTR	17–19
				ADQLYK	49–54
				EILAELTGR	104–112
				AAASTDYYK	207–215
				GDFIPGLR	217–224
				TREEIQEVR	274–282
				EIDVEVR	308–314
Pyruvate dehydrogenase (E1β component of PDC)	448581	35,765	16	LQVTVR	1–6
				DEKVFLLGEEVAQYDGAYK	20–38
				DFLIPLGK	190–197
				ILEDNSVPQVK	307–317
				DIIFAIK	318–324

[a] MS/MS ion search was performed using the following parameters: peptide tolerance ±1 Da, MS/MS tolerance ±0.5 Da, monoisotopic mass, one missed cleavage.
[b] Value from the NCBI protein database.

old rat hearts were used to determine total PDK activity, PDK-1 content, and the mRNA levels of PDK-2 and PDK-4 as described above (see Materials and methods). As shown in Figs. 3C and D, we found no age-related alterations in either PDK activity or PDK-1 content. However, PDK-4 mRNA decreased significantly ($P < 0.05$) by 57% in old rat hearts (Fig. 3E), while PDK-2 mRNA decreased by 42% ($P = 0.074$). Together, these analyses indicate that aging affects heart PDK-4 mRNA levels, to a lesser extent PDK-2 mRNA, while PDK-1 protein expression remains unaffected.

A dedicated pyruvate dehydrogenase phosphatase (PDP-1 and to a lesser extent PDP-2) catalyzes the dephosphorylation of E1α in skeletal and heart muscle, thereby re-activating PDC. The expression of PDP-1 is viewed as a means to control the level of activated PDC in response to nutritional and pathological conditions. We sought to determine whether the relative increase in active PDC in old rats was due to the differential gene transcription of PDP-1 and PDP-2 in the heart. To this end, PDP-1 and PDP-2 mRNA levels were measured by RT-PCR from total RNA extracts of young and old rat hearts. The results showed that mRNA levels were unchanged among age groups (Figs. 3F and G). Overall, these results suggest that the age-related decrease in PDC phosphorylation results from a decline in PDK-4 expression (possibly PDK-2 as well) with no change in PDP status.

Kinetic characteristics of PDC and fluoropyruvate inhibition

In the absence of any age-associated changes to PDC levels, we sought to determine whether the increased PDC activity in old rat hearts was linked to changes in kinetics of the enzyme complex. An assessment of Michaelis–Menten kinetic parameters for PDC when pyruvate concentration was varied revealed that PDC in old rat hearts exhibits a lower K_m for pyruvate than that seen in mitochondria from young rats. Analysis using a reciprocal plot of $1/V$ versus 1/pyruvate showed that the K_m was 1.6-fold lower in old (0.05 mM pyruvate) compared to young rats (0.13 mM). This change indicates a greater affinity of PDC in old rat hearts for its substrate (Fig. 4A). This age-associated increased affinity for pyruvate was further illustrated when fluoropyruvate, a competitive inhibitor, was allowed to compete with pyruvate for binding to PDC (Fig. 4B). PDC from old rat hearts showed a greater ($P \leqslant 0.05$) resiliency toward fluoropyruvate inhibition than PDC from young rat hearts (Fig. 4C).

Citrate synthase activity and kinetics

To determine if the increased kinetics and substrate affinity displayed by PDC and KGDC [20] were specific for these enzymes or were general to mitochondrial bioenergetic enzymes, CS activity and kinetics were

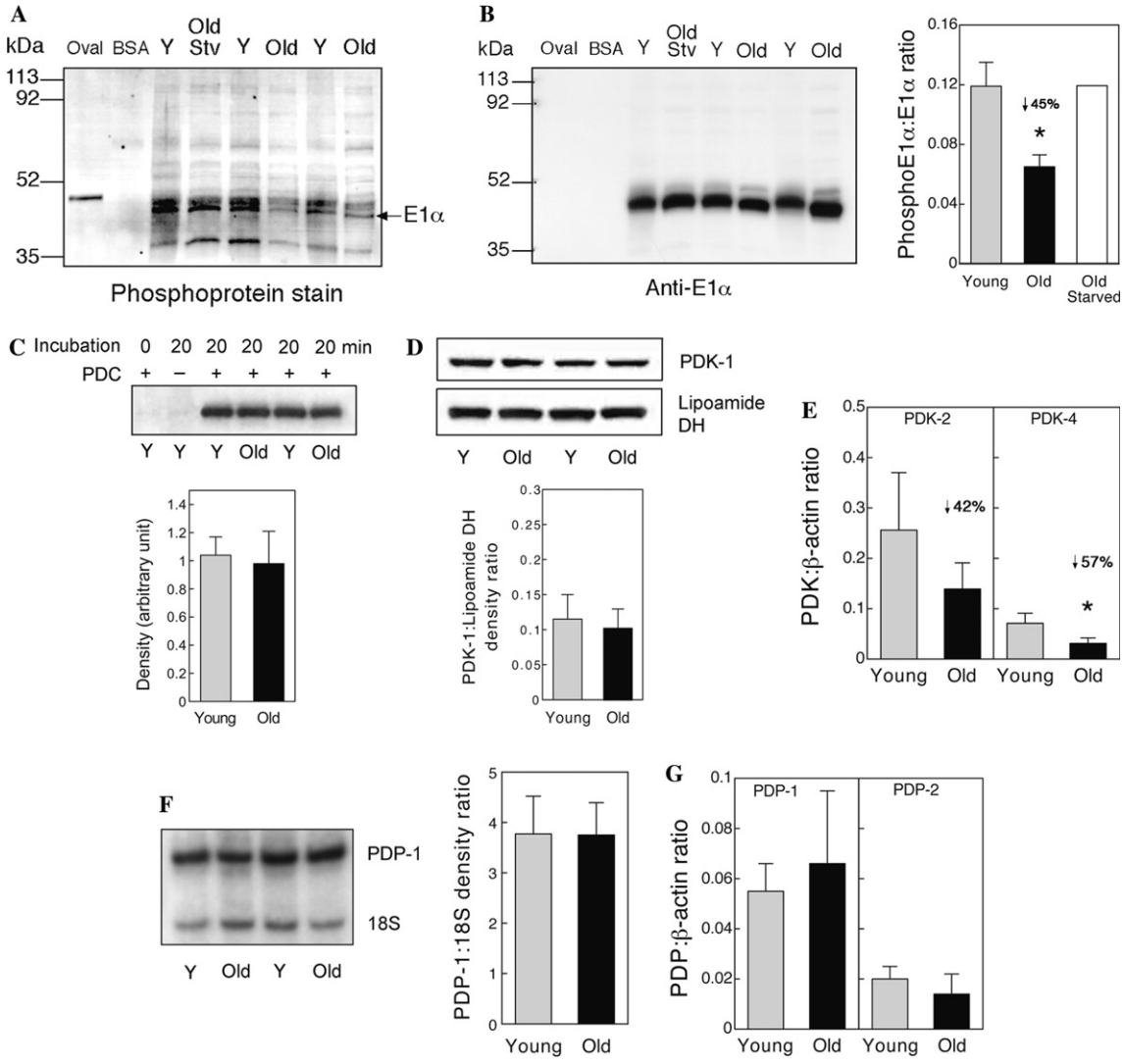

Fig. 3. Age-related changes to cardiac PDC phosphorylation, PDC kinase (PDK), and phosphatase (PDP) status in F344 rats. (A) Extent of protein phosphorylation in heart mitochondria isolated from young (Y), old (Old), and old 24-h starved (Old Stv) rats as determined with Pro-Q Diamond phosphoprotein blot stain, showing the location of the E1α enzymatic component of PDC (Oval, 0.2 μg ovalbumin; BSA, 0.2 μg bovine serum albumin). (B) Western blotting analyses of the E1 α-PDC in rat heart mitochondria using a monoclonal antibody to human E1α-PDC, and quantification of phosphorylated E1 α:total E1α ratio. Data are shown as means ± SD for 3 young and 3 old rats, and the mean of 2 old rats starved for 24 h (*indicates statistical significance, $P < 0.01$, between young and old rats). (C) PDK activity was measured as the initial rate of incorporation of [^{32}P]phosphate into the E1α component of porcine PDC catalyzed by rat heart mitochondria. (D) Rat heart PDK-1 content was determined by immunoblotting using antibodies to human PDK-1 and lipoamide dehydrogenase as loading control. (E) Heart mRNA levels of PDK-2 and PDK-4 isoforms were quantified by real-time RT-PCR from total RNA extracts of rat myocardium. (F) Heart PDP-1 mRNA levels as quantified by duplex RT-PCR using ribosomal 18S mRNA as an internal standard. (G) Heart mRNA levels of PDP-1 and PDP-2 as determined by real-time RT-PCR using β-actin as an internal standard. Data (C–G) are shown as means ± SD for 3–5 animals per age class (*indicates statistical significance, $P \leqslant 0.05$, between age class).

measured. Results show that CS activity and kinetic parameters were not significantly ($P > 0.05$) different between age groups (Figs. 5A and B).

Discussion

In the heart, mitochondrial oxidative metabolism provides the bulk of the ATP consumed during contraction and relaxation. Because the heart contains little ATP reserves, high-energy phosphate production is continuously dependent upon the efficiency of raw fuel conversion to reduced pyridine nucleotides generated in the mitochondria by various pathways, including pyruvate oxidation, β-oxidation, and the citric acid cycle. Multiple indices of mitochondrial bioenergetics decline in aging mammals, including the uptake and catabolism of long-chain fatty acids, leading to the decline of metabolic intermediates seen in F344 rat hearts (Fig. 1). Yet, the myocardium is, in part, able to compensate for these

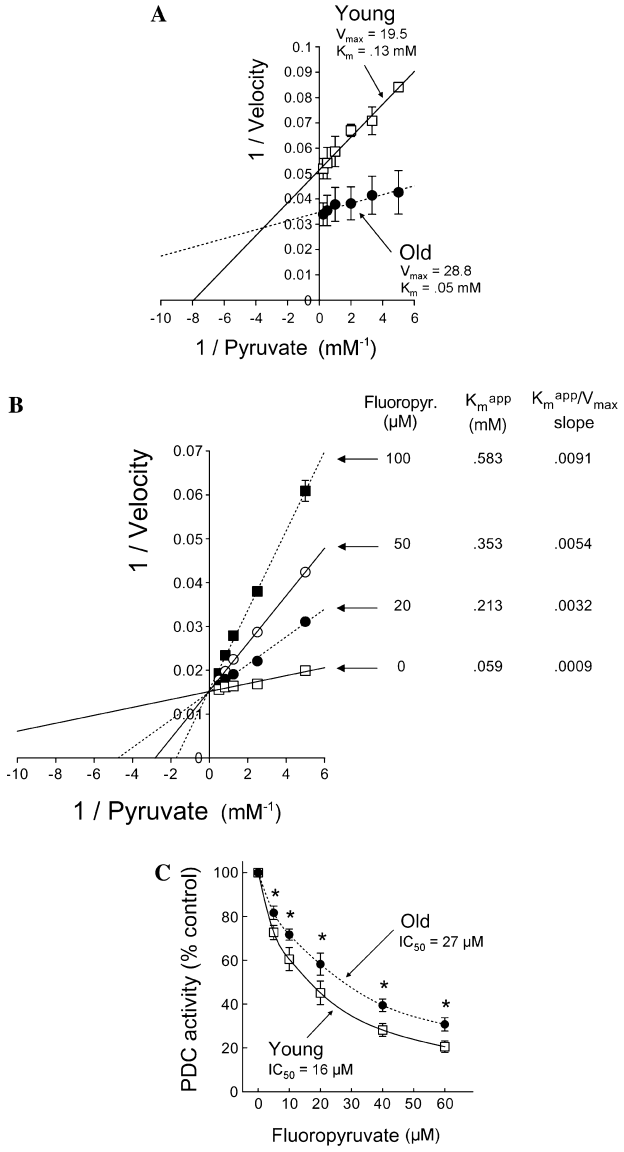

Fig. 4. Age-related changes to the kinetic characteristics of rat heart PDC. (A) K_m and V_{max} were derived from the Lineweaver–Burk double-reciprocal representation of the initial velocity of rat heart PDC. Given the hyperbolic profile of the initial velocity as a function of pyruvate concentration (0.2–4 mM), the reaction catalyzed by PDC was considered to follow Michaelis–Menten kinetics. Data are shown as means ± SD for 4 animals per age class. (B) Lineweaver–Burk plot showing the competitive inhibition of purified porcine heart PDC (5 mU) by fluoropyruvate (0–100 μM). The values of the intercepts (K_m^{app}) and slopes (K_m^{app}/V_{max}) were obtained graphically at each concentration of inhibitor. Data are shown as means ± SD for three experiments. (C) Age-dependent inhibition of rat heart PDC by fluoropyruvate. The greater affinity (lower K_m) of old rat PDC for its substrate, pyruvate (0.4 mM), is herein further evidenced by the greater resiliency (higher IC_{50}) toward the competitive inhibitor, fluoropyruvate. Data are shown as means ± SD for 5 animals per age class (*indicates statistical significance, $P \leqslant 0.05$, between age class).

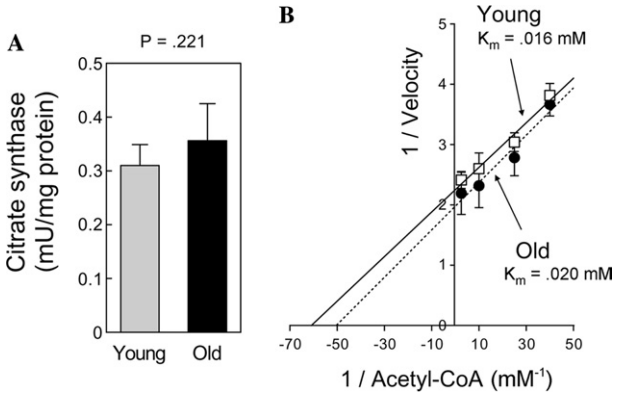

Fig. 5. Cardiac citrate synthase (CS) activity and kinetic parameters are unchanged between young and old rats. CS activity and kinetics were measured in isolated mitochondria. (A) CS activity was determined by monitoring the reduction of DTNB at 412 − 350 nm for 2 min at 30 °C. One CS unit refers to 1 mmol DTNB reduced per minute. Data are shown as means ± SD for 5 animals per age class. (B) CS kinetics was measured by varying acetyl-CoA concentration (25–400 μM) and plotting the initial velocity according to Lineweaver–Burk representation. Data are shown as means ± SD for 4 animals per age class.

alterations and thus maintain an adequate energy pool to allow the heart to function. Ultimately, the heart of senescent rats performs less work and utilizes less oxygen in proportion to tissue mass, but the ratio of oxygen consumed to the ventricular pressure developed remains unaltered [21].

The data presented in this study provide new evidence that PDC from old rat hearts catalyzes the decarboxylation of pyruvate with a greater efficiency compared to PDC in young rat hearts. This age-related change is viewed as a compensatory mechanism to maintain adequate NADH levels over a wide range of pyruvate concentrations, which would otherwise decline due to the loss of long-chain fatty acid oxidation. It also supports the view of a switch from fatty acid β-oxidation to carbohydrate catabolism for energy production [9]. To this end, cardiac mitochondria actively take up pyruvate originating in the cytosol by glycolysis and oxidize it via the PDC. The reversible activation of PDC represents the point of control of carbohydrate oxidation. Glucose-derived pyruvate provides 10–30% of the energy produced by the intact young working heart, but this share increases markedly with age. In addition to glucose-derived pyruvate, pyruvate is generated from lactate or taken up from the circulation all channel through PDC. Collectively, these carbohydrate sources provide 50–60% of acetyl-CoA entering the citric acid cycle; a contribution highly correlated with PDC stimulation [11].

We recently showed that KGDC, the rate-determining, NADH producing enzyme of the citric acid cycle, exhibited a comparable compensation as seen with PDC in old F344 rat hearts, i.e., a higher V_{max} and a lower K_m compared to their young counterparts [20]. It is worth noting that PDC and KDGC share multiple structural similarities. This age-related change in kinetic parameters, however, did not affect all enzymes involved

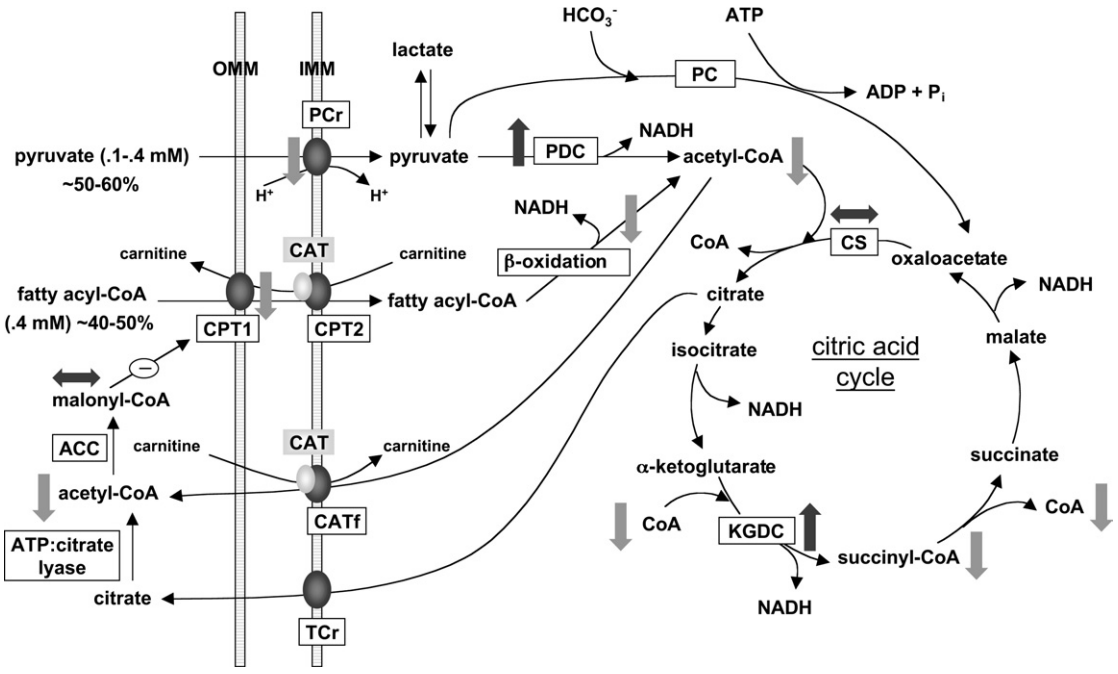

Fig. 6. Overall age-related changes to cardiac bioenergetics. ACC, acetyl-CoA carboxylase; CAT, carnitine acyl translocase; CATf, carnitine acyl transferase; CS, citrate synthase; CPT1, carnitine palmitoyl transferase 1; CPT2, carnitine palmitoyl transferase 2; IMM, inner mitochondrial membrane; KGDC, α-ketoglutarate dehydrogenase complex; OMM, outer mitochondrial membrane; PCr, pyruvate carrier; PC, pyruvate carboxylase; and PDC, pyruvate dehydrogenase complex.

in bioenergetics. The V_{max} and K_m of citrate synthase (CS), the initial enzyme of the citric acid cycle, were unchanged between age groups (Fig. 6). Like PDC and KGDC, CS catalyzes an irreversible reaction, but only displays modest control over the flux of substrates through the energy production pathway. This suggests that CS does not take part in the compensatory maintenance of mitochondrial bioenergetics in the aging rat heart.

Herein, we provide further insight into the regulation of PDC in old rat myocardium. PDC activity is modulated by various factors, including allosteric regulation by acetyl-CoA and NADH, and stimulation by Ca^{2+} and Mg^{2+} [22]. The effects of these organic and inorganic regulators are mediated by a dedicated kinase (PDK) and phosphatase (PDP) that modify the phosphorylation state of PDC. PDK phosphorylates three serine residues of the E1α component of PDC, thereby inactivating PDC. PDK activity depends on intramitochondrial ratios of CoA/acetyl-CoA, NAD^+/NADH, ADP/ATP, as well as on the concentration of pyruvate. Dephosphorylation and subsequent activation of PDC is catalyzed by a Mg^{2+}-dependent, Ca^{2+}-stimulated serine/threonine PDP. Ca^{2+} promotes the association of PDP with PDC, which stimulates dephosphorylation. To persist in vitro, altered PDC kinetics must result from a stable conformational change of the enzyme complex itself, such as the one induced by phosphorylation/dephosphorylation, because dilution and solubilization of mitochondria prior to assaying PDC activity disrupt the loose binding of NADH and acetyl-CoA. Indeed, we found that the age-related activation of heart PDC correlated with a decrease in E1α phosphorylation, suggesting the further involvement of PDK and/or PDP.

Aging of the heart influenced the expression profile of a specific PDK isoform (PDK-4) with no change to either PDP isoforms. The heart can express three isotypes of PDK (PDK-1, PDK-2, and PDK-4) [23] and both PDP isoforms (PDP-1 [24] and PDP-2). PDK-1 is expressed predominantly in cardiac muscle, PDK-2 is expressed ubiquitously, while PDK-4 is moderately expressed in the heart, lung, liver, and skeletal muscle. Recombinant PDK isotypes have varying activities toward E1α, with PDK-1 being the most efficient, followed by PDK-4 and PDK-2 [24]. Because total heart PDK activity (which measures in vitro the maximal phosphorylation capacity of PDK-1, PDK-2, and PDK-4 combined) and heart PDK-1 content were unchanged between young and old rats, we speculate that the expression profile of the most abundant isoforms in the heart, i.e., PDK-1 and PDK-2, is not markedly altered by tissue senescence. However, the differing regulation of PDK isoforms by allosteric intermediates in vivo, such as acetyl-CoA, NADH, and pyruvate, may contribute to the age-dependent change to PDC activation. In particular, our data suggest that lipid-sensitive PDK-4 markedly impacts PDC phosphorylation state in old rat hearts. Assuming that PDK-4 protein content in

the heart correlates with its mRNA level, the age-related down-regulation of PDK-4 may explain PDC phosphorylation and activation states in F344 rats.

Since acetyl-CoA and NADH activate PDK, it has been proposed that the activation state of PDC is decreased under conditions of high acetyl-CoA (low CoA:acetyl-CoA ratio) and NADH (low NAD^+:NADH). When fatty acids are oxidized, acetyl-CoA is produced and the CoA:acetyl-CoA ratio decreases, which in turn inhibits PDC. We found that the steady-state levels of acetyl-CoA decline 31% in old compared to young rat hearts. This suggests that acetyl-CoA down-regulates PDC by activating PDK in young rats only. Among the PDK isoforms found in the heart, PDK-1 is thought to be the most sensitive to acetyl-CoA activation [23]. But if PDK-1 was, indeed, primarily involved in the down-regulation of PDC in young rat hearts, we showed that this effect was independent of PDK-1 expression level, and suggests that alternative isoforms, i.e., PDK-4 and PDK-2, are also stimulated by acetyl-CoA.

Various nutritional conditions and pathological disorders have been shown to produce a stable increase in PDK activity. During starvation it is believed that heightened PDK activity allows conservation of carbohydrate fuels for tissues [25–28]. Changes in PDK expression can be achieved not only in response to starvation but also in response to a change in dietary composition, hormonal status, or developmental stage. By responding to lipid status, it has been proposed that PDK-4 facilitates fatty acid oxidation by sparing pyruvate [29]. PDK-4 up-regulation in skeletal muscle correlates with the use of lipid-derived fuels as respiratory substrates in high-fat fed rats [26]. Peroxisome-proliferator-activated receptor α (PPARα) was proposed to be the link between high-fat feeding and PDK-4 up-regulation in skeletal muscle and to a lesser extent in cardiac muscle [30]. At times of low lipid-derived substrate availability and decreased PPARα levels, such as documented for the aging heart [31], one would expect PDK-4 to be down-regulated. This view is, indeed, supported by our data showing a 57% decrease ($P < 0.05$) of PDK-4 mRNA levels in old rat hearts.

In addition to a conformational change induced by phosphorylation/dephosphorylation, heart senescence may be associated with changes to the PDC composition itself. Crucial to PDC activity is the concerted action of five catalytic components (E1α, E1β, E2, E3, and E3-binding protein), each present as multiple copies per complex. But, thus far, there is no evidence to suggest that aging affects PDC composition, nor has it been shown that modification of its composition, by addition or subtraction of enzymatic components, would alter kinetics.

Malonyl-CoA is believed to constitute a fuel sensor involved in cross-talk between fatty acid and glucose metabolism [32]. Stimulation of PDC will increase glucose oxidation, and mitochondrial acetyl-CoA, and citrate levels will rise, which serve as precursors of cytosolic acetyl-CoA. Cytosolic citrate and acetyl-CoA activate acetyl-CoA carboxylase (ACC), which produces malonyl-CoA. Under these conditions, fatty acid oxidation is suppressed by the action of malonyl-CoA on CPT-1. CPT-1β is primarily expressed in adult rat skeletal and cardiac muscle, and this isotype is strongly inhibited malonyl-CoA ($K_i \approx 0.02$ μM [32]). However, it is presently unclear how malonyl-CoA actually influences CPT-1β activity in vivo as physiological malonyl-CoA levels are far above the K_i of the enzyme. Regardless, under conditions of impaired uptake of fatty acids as seen in old rat hearts, the stimulation of PDC might adversely raise the steady-state levels of malonyl-CoA and further inhibit fatty acid oxidation. Malonyl-CoA levels in the heart were correlated ($r = 0.699$, $P = 0.036$) with cardiac acetyl-CoA levels, suggesting that malonyl-CoA derives from acetyl-CoA. Cardiac levels of malonyl-CoA reported in this study in young rats are comparable to previously documented values of 4–5 nmol g^{-1} wet weight [33,34]. Despite higher PDC activity, cardiac malonyl-CoA levels were slightly lower (−14%, $P > 0.05$) in old rats, suggesting that PDC-induced, malonyl-CoA-driven inhibition of CPT-1β contributes marginally to the decreased utilization of fatty acid by the aging heart.

In summary, aging of the myocardium is associated with adaptive changes to PDC kinetics, affecting V_{max} and K_m for pyruvate and leading to enhanced catalytic efficiency with no change in protein expression. These changes mimic those of old rat heart KGDC, an enzyme complex exhibiting broad structural similarities with PDC. Overall, this study suggests that potentially detrimental effects of tissue senescence on NADH production are offset by adaptive mechanisms in the form of increased catalytic efficiency of rate-determining bioenergetic enzymes, thereby compensating for lower substrate availability.

Acknowledgments

This work was supported by the Collins Medical Trust (R.M.) and National Institute on Aging Grant RIAG17141A (T.M.H.). We thank Brian Dixon for providing β-actin primers and Steven Lawson for critically reading the manuscript.

References

[1] A.M. Katz, Cellular mechanisms of heart failure, Am. J. Cardiol. 62 (1988) 3A–8A.
[2] F. Carré, F. Rannou, C. Sainte Beuve, B. Chevalier, J.M. Moalic, B. Swynghedauw, D. Charlemagne, Arrythmogenicity of the hypertrophied and senescent heart and relationship to membrane

proteins involved in the altered calcium handling, Cardiovasc. Res. 27 (1993) 1784–1789.
[3] D.D. Tresch, M.F.J. McGough, Heart failure with normal systolic function: a common disorder in older people, Am. Geriatr. Soc. 43 (1995) 1035–1042.
[4] W.S. Colucci, Molecular and cellular mechanisms of myocardial failure, Am. J. Cardiol. 80 (1997) 15L–25L.
[5] A. Haunstetter, S. Izumo, Apoptosis: basic mechanisms and implications for cardiovascular disease, Circ. Res. 82 (1998) 1111–1129.
[6] T.N. James, Normal and abnormal consequences of apoptosis in the human heart, Annu. Rev. Physiol. 60 (1998) 309–325.
[7] R. Hansford, Bioenergetics in aging, Biochim. Biophys. Acta 726 (1983) 41–80.
[8] G. Paradies, F.M. Ruggiero, Age-related changes in the activity of the pyruvate carrier and in the lipid composition in rat-heart mitochondria, Biochim. Biophys. Acta 1016 (1990) 207–212.
[9] J.B. McMillin, G.E. Taffet, H. Taegtmeyer, E.K. Hudson, C.A. Tate, Mitochondrial metabolism and substrate competition in the aging Fischer rat heart, Cardiovasc. Res. 27 (1993) 2222–2228.
[10] G. Paradies, G. Petrosillo, M.N. Gadaleta, F.M. Ruggiero, The effect of aging and acetyl-L-carnitine on the pyruvate transport and oxidation in rat heart mitochondria, FEBS Lett. 454 (1999) 207–209.
[11] S. Lloyd, C. Brocks, J.C. Chatham, Differential modulation of glucose, lactate, and pyruvate oxidation by insulin and dichloroacetate in the rat heart, Am. J. Physiol. Heart Circ. Physiol. 285 (2003) H163–H172.
[12] R. Hansford, Lipid oxidation by heart mitochondria from young adult and senescent rats, Biochem. J. 170 (1978) 285–295.
[13] R. Hansford, F. Castro, Age-linked changes in the activity of enzymes of the tricarboxylic acid cycle and lipid oxidation, and of carnitine content, in muscles of the rat, Mech. Ageing Dev. 19 (1982) 191–201.
[14] R. Bünger, R.T. Mallet, Mitochondrial pyruvate transport in working guinea-pig heart. Work-related vs. carrier-mediated control of pyruvate oxidation, Biochim. Biophys. Acta 1151 (1993) 223–236.
[15] P.J. Randle, Fuel selection in animals, Biochem. Soc. Trans. 14 (1986) 799–806.
[16] A. Demoz, A. Garras, D.K. Asiedu, B. Netteland, R.K. Berge, Rapid method for the separation and detection of tissue short-chain coenzyme A esters by reversed-phase high-performance liquid chromatography, J. Chromatogr. B 667 (1995) 148–152.
[17] J.W. Palmer, B. Tandler, C.L. Hoppel, Biochemical properties of subsarcolemmal and interfibrillar mitochondria isolated from rat cardiac muscle, J. Biol. Chem. 252 (1977) 8731–8739.
[18] D. Chretien, M. Pourrier, T. Bourgeron, M. Séné, A. Rötig, A. Munnich, P. Rustin, An improved spectrophotometric assay of pyruvate dehydrogenase in lactate dehydrogenase contaminated mitochondrial preparations from human skeletal muscle, Clin. Chim. Acta 240 (1995) 129–136.
[19] C.E. Doneanu, D.A. Griffin, E.L. Barofsky, D.F. Barofsky, An exponential dilution gradient system for nanoscale liquid chromatography in combination with MALDI or nano-ESI mass spectrometry for proteolytic digests, J. Am. Soc. Mass Spectrom. 12 (2001) 1205–1213.
[20] R. Moreau, S.-H.D. Heath, C.E. Doneanu, J.G. Lindsay, T.M. Hagen, Age-related increase in 4-hydroxynonenal adduct to rat heart α-ketoglutarate dehydrogenase does not cause loss of its catalytic activity, Antioxid. Redox Signal. 5 (2003) 517–527.
[21] G.M. Abu-Erreish, J.R. Neely, J.T. Whitmer, V. Whitman, D.R. Sanadi, Fatty acid oxidation by isolated perfused working hearts of aged rats, Am. J. Physiol. 232 (1977) E258–E262.
[22] J. Yan, J.E. Lawson, L.J. Reed, Role of the regulatory subunit of bovine pyruvate dehydrogenase phosphatase, Proc. Natl. Acad. Sci. USA 93 (1996) 4953–4956.
[23] M.M. Bowker-Kinley, W.I. Davis, P. Wu, R.A. Harris, K.M. Popov, Evidence for existence of tissue-specific regulation of the mammalian pyruvate dehydrogenase complex, Biochem. J. 329 (1998) 191–196.
[24] B. Huang, R. Gudi, P. Wu, R.A. Harris, J. Hamilton, K.M. Popov, Isoenzymes of pyruvate dehydrogenase phosphatase, J. Biol. Chem. 273 (1998) 17680–17688.
[25] P. Wu, J. Sato, Y. Zhao, J. Jaskiewicz, K.M. Popov, R.A. Harris, Starvation and diabetes increase the amount of pyruvate dehydrogenase kinase isoenzyme 4 in rat heart, Biochem. J. 329 (1998) 197–201.
[26] M.J. Holness, A. Kraus, R.A. Harris, M.C. Sugden, Targeted upregulation of pyruvate dehydrogenase kinase (PDK)-4 in slow-twitch skeletal muscle underlies the stable modification of the regulatory characteristics of PDK induced by high-fat feeding, Diabetes 49 (2000) 775–781.
[27] P. Wu, P.V. Blair, J. Sato, J. Jaskiewicz, K.M. Popov, R.A. Harris, Starvation increases the amount of pyruvate dehydrogenase kinase in several mammalian tissues, Arch. Biochem. Biophys. 381 (2000) 1–7.
[28] S.J. Peters, R.A. Harris, G.J.F. Heigenhauser, L.L. Spriet, Muscle fiber type comparison of PDH kinase activity and isoform expression in fed and fasted rats, Am. J. Physiol. Regulatory Integrative Comp. Physiol. 280 (2001) R661–R668.
[29] M.C. Sugden, K. Bulmer, M.J. Holness, Fuel-sensing mechanisms integrating lipid and carbohydrate utilization, Biochem. Soc. Trans. 29 (2001) 272–278.
[30] M.J. Holness, N.D. Smith, K. Bulmer, T. Hopkins, G.F. Gibbons, M.C. Sugden, Evaluation of the role of peroxisome-proliferator-activated receptor α in the regulation of cardiac pyruvate dehydrogenase kinase 4 protein expression in response to starvation, high-fat feeding and hyperthyroidism, Biochem. J. 364 (2002) 687–694.
[31] M. Iemitsu, T. Miyauchi, S. Maeda, T. Tanabe, M. Takanashi, Y. Irukayama-Tomobe, S. Sakai, H. Ohmori, M. Matsuda, I. Yamaguchi, Aging-induced decrease in the PPAR-α level in hearts is improved by exercise training, Am. J. Physiol. Heart Circ. Physiol. 283 (2002) H1750–H1760.
[32] J.D. McGarry, Travels with carnitine palmitoyltransferase 1: from liver to germ cell with stops in between, Biochem. Soc. Trans. 29 (2001) 241–245.
[33] J.D. McGarry, S.E. Mills, C.S. Long, D.W. Foster, Observations on the affinity for carnitine, and malonyl-CoA sensitivity, of carnitine palmitoyltransferase I in animal and human tissues. Demonstration of the presence of malonyl-CoA in non-hepatic tissues of the rat, Biochem. J. 214 (1983) 21–28.
[34] M. Saddik, J. Gamble, L.A. Witters, G.D. Lopaschuk, Acetyl-CoA carboxylase regulation of fatty acid oxidation in the heart, J. Biol. Chem. 268 (1993) 25836–25845.